Behavior of Ilmenite as Oxygen Carrier in Chemical-Looping Combustion

A. Cuadrat, A. Abad*, J. Adánez, L.F. de Diego, F. García-Labiano, P. Gayán

Instituto de Carboquímica (C.S.I.C.), Dept. of Energy & Environment, Miguel Luesma Castán, 4, Zaragoza, 50018, Spain

* e-mail: abad@icb.csic.es

ABSTRACT

For a future scenery where will exist limitation for CO_2 emissions, Chemical-Looping Combustion (CLC) has been identified as a promising technology to reduce the cost related to CO_2 capture from power plants. In CLC a solid oxygen-carrier transfers oxygen from the air to the fuel in a cyclic manner, avoiding direct contact between them. CO_2 is inherently obtained in a separate stream. For this process the oxygen-carrier circulates between two interconnected fluidized-bed reactors. To adapt CLC for solid fuels the oxygen-carrier reacts with the gas proceeding from the solid fuel gasification, which is carried out right in the fuel-reactor. Ilmenite, a natural mineral composed of $FeTiO_3$, is a low cost and promising material for its use on a large scale in CLC.

The aim of this study is to analyze the behavior of ilmenite as oxygen-carrier in CLC. Particular attention was put on the variation of chemical and physical characteristics of ilmenite particles during consecutive redox cycles in a batch fluidized-bed reactor using CH_4, H_2 and CO as reducing gases. Reaction with H_2 was faster than with CO, and near full H_2

conversion was obtained in the fluidized-bed. Lower reactivity was found for CH_4. Ilmenite increased its reactivity with the number of cycles, especially for CH_4. The structural changes of ilmenite, as well as the variations in its behavior with a high number of cycles were also evaluated with a 100 cycle test using a $CO+H_2$ syngas mixture. Tests with different H_2:CO ratios were also made in order to see the reciprocal influence of both reducing gases and it turned out that the reaction rate is the sum of the individual reaction rates of H_2 and CO. The oxidation reaction of ilmenite was also investigated. An activation process for the oxidation reaction was observed and two steps for the reaction development were differenced. The oxidation reaction was fast and complete oxidation could be reached after every cycle. Low attrition values were found and no defluidization was observed during fluidized-bed operation. During activation process, the porosity of particles increased from low porosity values up to values of 27.5%. The appearance of an external shell in the particle was observed, which is Fe enriched. The segregation of Fe from TiO_2 causes that the oxygen transport capacity, R_{OC}, decreases from the initial R_{OC} = 4.0% to 2.1% after 100 redox cycles.

1. Introduction

At present there is a general assent on the need of reducing the emissions of the greenhouse gas CO_2 in order to restrain climate change. Anthropogenic CO_2 is mainly generated in combustion of fossil fuels, which are foreseen to provide about 80% of the overall world consumption of energy for the next several decades. For the power generation and heat supply sector, emissions were 12.7GtCO_2-eq in 2004, which is 26% of total CO_2-eq emissions. When regarding the energy-related CO_2 emissions by fuel type, coal use generated 39% of the emissions in 2004 and it is estimated that the percentage in 2030 will rise up to 43% [1,2]. Among the different opportunities to reduce the anthropogenic CO_2 emissions, the

development of technologies to capture CO_2 from fossil fuel uses and to store it permanently has been identified as a relevant option in the future, being the implementation of these technologies more feasible and readily in stationary power plants.

In this context, Chemical-Looping Combustion (CLC) is one of the most promising technologies to carry out the CO_2 capture at a low cost [3,4,5]. CLC is based on the transfer of the oxygen from air to the fuel by means of a solid oxygen-carrier that circulates between two interconnected fluidized-beds: the fuel- and the air-reactor [6]. In the fuel-reactor the oxygen-carrier is reduced through oxidation of the fuel. Afterwards the oxygen-carrier is directed to the air-reactor, where it is again regenerated, as the inlet air flow reacts with the solid. The net chemical reaction is the same as at usual combustion with the same combustion heat released.

Important progress has been made in CLC with natural gas to date. Several authors have successfully demonstrated the feasibility of this process in different CLC prototypes in the 10-140 kW_{th} range using oxygen-carriers based on NiO [7,8,9,10] and CuO [11].

But increasing interest is found about the application of CLC using coal as fuel, regarding the intensive use of this fuel. There are two possibilities for the use of the CLC technology with coal. The first one is to carry out previous coal gasification and subsequently to introduce the produced gas in the CLC system [12]. In this option pure oxygen is needed to carry out the gasification to produce syngas with no N_2. Thus, the extra gasifier and the production of pure oxygen would entail an additional energetic cost. Simulations performed by Jin and Ishida [13] and Wolf et al. [14] showed that this process has the potential to achieve an efficiency of about 5-10% points higher than a similar combined cycle that uses conventional CO_2 capture technology. Several oxygen-carriers based on Ni, Cu, Fe and Mn oxides have shown good

reactivity with syngas components, i.e. H_2 and CO [15,16], and the use of syngas in a CLC system has been successfully accomplished in 300-500 W_{th} continuously operated reactors [17-21].

The second possibility for the use of coal in a CLC is the direct combustion in the CLC process [22,23]. The reactor scheme of the direct CLC process with solid fuels is shown in Figure 1. In this option coal is physically mixed with the oxygen-carrier in the fuel-reactor and the carrier reacts with volatiles and the gas product of coal gasification, where H_2 and CO are main components. Eqs. (1) to (5) express generally the reactions that take place in the fuel-reactor, being (3) to (5) the oxygen-carrier reduction reactions with the main products of coal devolatilization and gasification. The oxygen-carrier is subsequently introduced in the air-reactor where it is re-oxidized following reaction (6). Me_xO_y and Me_xO_{y-1} are the oxidized and reduced form, respectively, of the oxygen-carrier.

$$\text{Coal} \rightarrow \text{Volatiles} + \text{Char} \quad (1)$$

$$\text{Char} + H_2O \rightarrow CO + H_2 \quad (2)$$

$$CH_4 + 4\ Me_xO_y \rightarrow CO_2 + 2\ H_2O + 4\ Me_xO_{y-1} \quad (3)$$

$$H_2 + Me_xO_y \rightarrow H_2O + Me_xO_{y-1} \quad (4)$$

$$CO + Me_xO_y \rightarrow CO_2 + Me_xO_{y-1} \quad (5)$$

$$2\ Me_xO_{y-1} + O_2 \rightarrow 2\ Me_xO_y \quad (6)$$

The stream of combustion gases from the fuel-reactor contains primarily CO_2 and H_2O. Water can be easily separated by condensation and a highly concentrated stream of CO_2 ready for sequestration is achieved. The gas stream from the air-reactor is oxygen-depleted and consists in N_2 and some unreacted O_2. The CO_2 capture is inherent to this process, as the air does not

get mixed with the fuel, and no additional costs or energy penalties for gas separation are required.

The gasification process is expected to be the limiting step in the fuel-reactor, so the stream of solids exiting the fuel-reactor could contain some unconverted char together with the oxygen-carrier. Thus, an additional carbon stripper is necessary to separate char particles from oxygen-carrier particles, reducing the carbon transferred from the fuel- to the air-reactor. As a consequence of the ashes present in the solid fuel, the draining of ashes from the system is necessary to avoid its accumulation in the reactors. This drain stream will also contain some oxygen-carrier. It is therefore expected that the active life of this material would be limited by the losses with the drain stream rather than by its degradation.

Low cost of the carrier is rather desirable for its use with coal, as it is predictable a partial loss together with the coal ashes when removing them from the reactor to avoid their accumulation in the system. The use of natural minerals for this option seems to be very interesting, being ilmenite an appropriate material [24-28].

As for gaseous fuels, suitable oxygen-carriers for solid fuels in the CLC process must have high selectivity towards CO_2 and H_2O, enough oxygen transport capacity, high reactivity, high mechanical strength, attrition resistance and agglomeration absence. All these properties must be maintained during many reduction and oxidation cycles. Ilmenite has shown to be a low cost suitable material to be used for solid fuel combustion in a CLC system. Leion et al. [29,30] analyzed the reactivity of ilmenite in a batch fluidized-bed and ilmenite gave high conversion of H_2 and CO but moderate conversion of CH_4. This carrier has been already used in both gaseous and solid fuels [24-27,31]. Ilmenite is mainly composed of $FeTiO_3$

($FeO{\cdot}TiO_2$), where iron oxide is the active phase that behaves as the oxygen-carrier. There are a few recent studies made and a good performance of ilmenite at different levels as oxygen-carrier in CLC has been observed. For solid fuels combustion, the ilmenite reacted just as well as a synthetic Fe_2O_3-based oxygen-carrier. They also observed a gain in the ilmenite reactivity as increasing the redox cycles until a maximum reaction rate was reached and maintained with the cycles, which has been also seen and proven after 100 redox cycles in TGA for various gaseous fuels by Adánez et al. [32], as well as when using solid fuels in batch testing [33]. Berguerand et al. [24,25] operated a 10 kW_{th} chemical-looping combustor using South African coal and petroleum coke as solid fuels. They used the same batch of ilmenite particles for about 100 hours under different conditions and the oxygen-carrier maintained its good properties throughout operation. This was confirmed by Cuadrat et al. [27] in their study of the Fuel Reactor and the effect of operational variables in the efficiency of the process. The encouraging results to date obtained indicate that there is still further research to be carried out. Besides, all research to date about ilmenite performance as oxygen-carrier has analyzed only the reduction step.

The aim of this work is to investigate ilmenite as oxygen-carrier in a CLC system and the effect of the number of cycles on its reactivity with the main gases from coal pyrolysis and gasification, that is, CH_4, CO and H_2. In addition, this study includes an assessment on the oxidation step and its changes after many redox cycles. Consecutive reduction-oxidation cycles were carried out in a batch fluidized-bed reactor using CH_4, CO and H_2 as reducing agents. To analyze the activation process a characterization of the initial and reacted samples of oxygen-carrier was also done. Further fluidized-bed tests were carried out using syngas as fuel. The structural changes of ilmenite, as well as the variations in its behavior with a high number of cycles were also evaluated with a 100 cycle test using a H_2+CO syngas mixture.

Tests with different H_2:CO ratios were also made in order to see the reciprocal influence of both reducing gases in the reaction rate.

2. Experimental section

2.1. Oxygen-carrier material

Ilmenite is a common mineral found in metamorphic and igneous rocks. The ilmenite used is a concentrate from a natural ore. Fresh particles have been exposed to thermal pre-treatment at 950ºC in air during 24 hours, since it improves its performance as oxygen-carrier [30,31]. Table 1 shows the main properties for calcined ilmenite. The XRD analysis of calcined ilmenite revealed that Fe_2TiO_5 and TiO_2 were the major components, with minor amount of Fe_2O_3. The composition of calcined ilmenite was 55.5 wt% Fe_2TiO_5, 10.6 wt% Fe_2O_3, 28.4wt% TiO_2 and 5.5 wt% of other inert compounds. The crushing strength was measured by using a Shimpo FGN-5 crushing strength apparatus. The final measure was obtained from the average of at least 20 different measurements. The values of crushing strength obtained for the initial ilmenite are similar to other Fe-based oxygen-carriers [34]. Mercury porosimetry of initial ilmenite exhibits low porosity development. Table 1 also shows the main properties of the so-called activated ilmenite. They are reacted particles after several redox cycles and undergo an increase in the reaction rate which will be discussed later.

2.2. Batch fluidized-bed reactor

Several reduction-oxidation cycles with different reducing gases were performed in a batch fluidized-bed to investigate the gas product distribution and the variation of chemical and physical properties of the ilmenite particles with the number of cycles.

Figure 2 shows the experimental setup. It consists of a system for gas feeding, a fluidized-bed reactor (55 mm I.D.), two filters that recovers the solids elutriated from the fluidized-bed working alternatively, and the gas analysis system. The whole fluidized-bed reactor is inside an electrically heated furnace. A detailed description of the apparatus and procedure can be found elsewhere [35]. The gas feeding system had different mass flow controllers connected to an automatic three-way valve. This allowed the feeding of the fuel gas (mixtures of CH_4, CO, CO_2, H_2, H_2O and N_2) during the reducing period and a mixture of air and N_2 for oxidation of ilmenite. Nitrogen was introduced between the two periods during 2 min to purge and avoid the contact between the fuel and the oxygen. For the supplying of the steam there is a liquid flow controller for water which is subsequently heated up and evaporated with a resistance heater and swept away by the rest of the reducing gas.

The differential pressure drop in the bed is measured by means of two pressure taps connected to the bottom and top of the reactor, and are used to detect possible agglomeration problems in the bed. The gas analysis system consists of several online gas analyzers. CH_4, CO and CO_2, dry basis concentrations are measured using non-dispersive infrared analysis (NDIR) and H_2 by thermal conductivity. O_2 concentration is determined using a paramagnetic analyzer. Water content, on wet basis is measured via Fourier Transform Infrared (FTIR Gasmet Cx-4000) analyzer. All data were collected by means of a data logger connected to a computer. The gas flow dispersion through the sampling line and the analyzers was corrected

for all the measured gas concentrations in order to obtain the actual concentration of the gases at the bed exit by a deconvolution method [19].

The total solids hold-up in the reactor was 500 g of precalcined ilmenite. The oxygen-carrier was exposed to alternating reducing and oxidizing conditions at a temperature of 1173 K. The reducing conditions of each experiment are shown in Table 2. 20-23 redox cycles with CH_4, CO and H_2 as reducing agents were performed to see the reaction and activation process of ilmenite with the main gases involved in the CLC process with coal. The behavior of the oxygen-carrier upon different syngas mixtures was also assessed. Together with H_2 and CO, both H_2O and CO_2 were introduced to accomplish the water-gas shift equilibrium at 1173 K. The reducing time in these tests was 240 s. A long 100 redox cycle test was performed with one of the syngas mixtures as reducing agent. All tests, except the CH_4 tests, accomplished that 50% of the inlet flow is a gaseous fuel mixture and the total inlet gas velocity was 0.30 m/s.

The reducing gas flows were chosen to have the same oxygen consumption. This condition was obtained by doubling the gas concentrations and fluidizing gas velocity for CO and H_2 in reference to what was used for CH_4. The flow for CO, H_2 and the syngas mixtures was 300 L_N/h, which was four times the flow of the introduced CH_4, 75 L_N/h. Considering a mean particle diameter of 212 μm, the minimum fluidization velocity for the calcined ilmenite particles at this temperature is 2.7 cm/s and the terminal velocity is 1.7 m/s. The gas velocities are 5 and 10 times the minimum fluidization velocity, respectively.

H_2O or CO_2 were added to the reducing gases because in the continuous real process the fuel-reactor will be at a steam and CO_2 enriched atmosphere, and also to prevent carbon formation.

The thermodynamic equilibriums indicate that with the gas mixtures of these experiments the ilmenite particles can get reduced further than Fe_3O_4 + $FeTiO_3$. Fe_2TiO_5 in ilmenite should be reduced to $FeTiO_3$ and Fe_2O_3 should be only reduced up to Fe_3O_4 to reach full conversion of the reducing gases [32].The reducing times are however short and ilmenite was not in any case converted further than the wanted species, i.e, no further reduction of Fe_3O_4 to FeO or Fe.

The subsequent oxidations were carried out with diluted air (10% O_2) to avoid a high temperature increase in the reactor because the heat released during the exothermic oxidation. The oxidation period lasted until full oxidation of the oxygen-carrier.

3. Data evaluation

The oxygen transport capacity of the ilmenite, R_{OC}, is defined as the mass fraction of oxygen that can be used in the oxygen transfer and calculated as $R_{OC} = (m_{ox} - m_{red})/m_{ox}$, where m_{ox} and m_{red} are the mass of the most oxidized and reduced form of the oxygen-carrier, respectively. The oxygen transport capacity, for ilmenite is the oxygen transferred in its reduction from Fe_2TiO_5+Fe_2O_3 to $FeTiO_3$+Fe_3O_4, as later will be discussed.

From the gas product distribution, it is possible to know the rate of oxygen transferred, $r_0(t)$, from ilmenite to the fuel gas in case of the reduction reaction, and from the oxygen in the air to ilmenite in case of the oxidation reaction, as a function of reaction time using Eqs. (7) to (10):

For CH_4: $$r_0(t) = (x_{CO} + 2x_{CO_2} + x_{H_2O})_{out} \cdot F_{out} - (x_{H_2O})_{in} \cdot F_{in} \quad (7)$$

For CO: $$r_0(t) = (x_{CO_2})_{out} \cdot F_{out} - (x_{CO_2})_{in} \cdot F_{in} \quad (8)$$

For H_2: $$r_0(t) = (x_{H_2O})_{out} \cdot F_{out} - (x_{H_2O})_{in} \cdot F_{in} \quad (9)$$

For O_2: $$r_0(t) = 2 \cdot (x_{O_2})_{out} \cdot F_{out} - 2 \cdot (x_{O_2})_{in} \cdot F_{in} \quad (10)$$

where F_{in} and F_{out} are the molar flows of the respectively inlet and outlet gas streams and x_i the molar fraction of the gas i.

The mass based conversion of ilmenite in the fluidized-bed, ω, indicates only the oxygen transfer and is independent of the oxygen transport capacity of the oxygen-carrier. It can be calculated for the reduction and oxidation reactions as:

For reduction: $$\omega(t) = 1 - \frac{M_O}{m_{ox}} \int_{t_{r,0}}^{t} r_0(t)dt \quad (11)$$

For oxidation: $$\omega(t) = \omega_{f,red} - \frac{M_O}{m_{ox}} \int_{t_{r,0}}^{t} r_0(t)dt \quad (12)$$

where M_O is the molecular mass of oxygen, $t_{r,0}$ is the initial time when the considered reaction begins and $\omega_{f,red}$ is the final conversion of ilmenite reached in the previous reduction. The experimental rate of conversion, $(d\omega/dt)_{exp}$, is therefore obtained by means of Eq. (13):

$$\left(\frac{d\omega}{dt}\right)_{exp} = \frac{M_O}{m_{ox}} r_0(t) \quad (13)$$

For comparison purposes among different experiments, the oxygen yield parameter is proposed, which gives the idea to what extend the fuel has been oxidized at each instant of the

reducing period. The oxygen yield, γ_O, is defined as the oxygen gained in the fuel for its oxidation divided by the oxygen needed to fully oxidize the fuel, according to Eq. (14):

$$\gamma_O(t) = \frac{r_0(t)}{(4x_{CH_4} + x_{CO} + x_{H_2})_{in} \cdot F_{in}} \tag{14}$$

A normalized rate index expressed in %/min is also used in this study to evaluate the reaction rates of all the gaseous fuels tested with ilmenite before and after the activation period, and also as a comparison parameter that has been previously used with other oxygen-carriers for CLC. It is defined as follows:

$$Rate\,index(\%/\min) = 60 \cdot 100\left(\frac{d\omega}{dt}\right)_{norm} = 60 \cdot 100\left(\frac{d\omega}{dt}\right)_{exp} \frac{P_{ref}}{P_m} \tag{15}$$

Where P_m is the average partial pressure of the gaseous fuel in the reactor, which is calculated with the coefficient of expansion of the gas mixture ε_g, and the partial pressures of the gaseous fuel at the reactor inlet and outlet, P_{in} and P_{out}, respectively, see Eq (16). P_m was calculated considering that the order of reaction is 1. P_{ref} is a reference partial pressure that has been used in previous studies and it is 0.15 [34] and is here used to be able to compare ilmenite to other previously oxygen-carriers used. This reference value would correspond to a gas conversion of 93% CH_4 and 99.9% for H_2 or CO, considering an inlet partial pressure of 1, that the mass transfer resistance between the bubble and emulsion phases in the fluidized bed reactor is small, that the reaction of the gaseous fuel is of first order and that there is no gas expansion.

$$P_m = \frac{(P_{in} - P_{out}) \Big/ (P_{in} + \varepsilon_g \cdot P_{out})}{\frac{(P_{out} - P_{in}) \cdot \varepsilon_g}{(P_{in} + \varepsilon_g \cdot P_{out})} + (1 + \varepsilon_g) \ln\left(\frac{P_{in} + \varepsilon_g \cdot P_{out}}{(1 + \varepsilon_g) P_{out}}\right)} \quad (16)$$

4. Results and discussion

4.1. Activation and reactivity with gaseous fuels: CH_4, CO and H_2

The experiments carried out in the fluidized-bed reactor allow the knowledge of the behavior of the ilmenite to oxidize CH_4, CO or H_2 during successive reduction-oxidation cycles. Figure 3 shows the CO_2 concentration in dry basis or H_2O concentration during consecutive reduction periods for experiments 1, 2 and 3, that is, tests using CH_4, CO and H_2 as reducing gases, respectively. The experimental conditions are gathered in Table 2. The corresponding maximum CO_2 or H_2O fractions if full combustion was reached are also represented. It can be seen that, for every tested reducing gas, there is an increase in the percentage of CO_2 and/or H_2O in the product gas with the cycles because ilmenite has a gradual gain in its reaction rate. After several redox cycles, ilmenite reactivity stabilizes and the CO_2 and/or H_2O concentrations achieve the highest values. After that, the outlet gas profiles could be considered rather the same from cycle to cycle and thus no further substantial activation of ilmenite was taking place. Therefore, there is a progressive activation process with the redox cycle number. It is noticeable the strong increase of the ilmenite reactivity with CH_4. These results are similar than those showed by Leion et al. during redox cycles of ilmenite in a fluidized-bed using CH_4 and 50% H_2 + 50% CO as reducing gases [29]. This was also observed by Abad et al. [38], for which reaction rate of ilmenite with CH_4 rises about 15 times after several redox cycles and activating.

An increase of the generated H_2O can be also seen when using H_2 as reducing agent (see Figure 3.c), but the activation of ilmenite can be slightly seen, since it oxidizes almost all the fuel fed in the reactor. Thus, the reaction rate of ilmenite in the bed was limited by the H_2 supply.

The product gas distribution of the gases at the reactor exit was obtained to evaluate the performance of ilmenite on the conversion of CH_4, H_2 and CO, and its evolution with the cycle number.

As an example, Figure 4 shows the outlet product gas distribution for the 20^{th} cycle for experiment 1 using CH_4 as reducing agent. CO_2 and H_2O were formed just immediately after the introduction of the reducing gas to the reactor, but full conversion of the reducing gas was not obtained. The ilmenite mass based conversion, ω, as a function of the reaction time is also displayed. The unconverted fuel gas increased as the conversion increased, because the rate of oxygen transference decreased as there was continuous oxygen depletion in ilmenite. For CH_4 combustion is noticeable that most of unconverted gas is the selfsame CH_4 and almost no CO or H_2 were observed. This fact suggests that the reforming reaction of CH_4 with H_2O or CO_2 has low relevance in this system using ilmenite as oxygen-carrier. Furthermore, in previous studies with Fe-based oxygen-carriers, the majority of CH_4 converted goes to CO_2 and H_2O, but CO and H_2 also appear in variable amounts [[20,[31]. Thus, it can be assumed that reaction of CH_4 takes place with H_2 and CO as intermediate products. However in this case there was no H_2 or CO at the outlet because the possible generated H_2 and CO react faster with ilmenite than CH_4 and they were therefore consumed. The appearance of unconverted gases during the experimental tests did not mean that fuel gas could not be fully converted to

CO_2 and H_2O using ilmenite as oxygen-carrier, but a higher amount of ilmenite in the fluidized-bed reactor would be needed to fully convert the fuel gas at the experimental conditions, i.e. temperature and gas velocity. However, experiments with incomplete fuel conversion are required to analyze the reactivity of an oxygen-carrier in fluidized-bed experiments, so that the gas conversion is not limited by the fuel gas supply.

After reduction, ilmenite was regenerated by oxidation with diluted air until full oxidation of ilmenite was reached. During most of ilmenite oxidation period, the O_2 outlet concentration was zero because the oxygen was consumed by the oxidation reaction. Thus, ilmenite oxidation was limited by the supply of O_2 to the reactor. At the end of the oxidation period, the oxygen concentration rapidly increased until the inlet concentration.

Similar gas profiles were found with all redox cycles, except for differences on the fuel gas conversion with the cycle number. With CO as reducing agent, relevant amount of unreacted CO was found during the reducing periods. Ilmenite reacted faster with CO than with CH_4, but not as fast as with H_2. The conversion after 4 minutes of the 20^{th} reducing period was 0.982. That conversion meant that the oxygen-carrier was partially reduced, as the corresponding value for completely reduced ilmenite to $FeTiO_3$+Fe_3O_4 was lower: it was 0.965. XRD of completely reduced samples confirmed that the final species were $FeTiO_3$, Fe_2TiO_4 and Fe_3O_4.

The reactivity of the oxygen-carrier can be seen by means of the oxygen yield, γ_O. It shows the percentage of the fuel that has been oxidized at each instant of the reducing period. Thus, Figure 5 represents the oxygen yield vs. ilmenite mass based conversion for selected cycles during the activating period using CH_4, CO and H_2 as reducing agents. As expected, the

oxygen yield and the ilmenite mass based conversion reached in every cycle increases with the first number of cycles, as there is reactivity rise, and when ilmenite is active, γ_O stabilized in a maximum value. It can be seen, in the CO_2 and H_2O profiles as well as in the oxygen yield, that ilmenite undergoes an activation process.

The decrease seen in the oxygen yield for higher ilmenite conversions is due to its gradual oxygen depletion. The oxygen yield at the beginning of the first cycle was 10% and rose up to 56% in the twentieth cycle for CH_4 as reducing agent. γ_O for CO is lower than for H_2 because of the lower reactivity of ilmenite with CO, but it was higher than for CH_4, and reached values of 78%.

When using H_2 as reducing agent, a very low amount of unconverted H_2 was observed throughout the reducing period. Only for the first 3-4 cycles before the activation of the oxygen-carrier, the reaction was limited by the H_2 flow introduced in the system from the beginning of the reducing period. For later cycles ilmenite oxidizes almost all the H_2 at the beginning of the reductions, and further activation of ilmenite could not be seen, if happened. γ_O was as high as 98% at the beginning of the reducing period when ilmenite was activated. Ilmenite is very reactive with this gas, as it has already been proven in several studies. The conversion at the end of the reducing cycle was higher than with methane even after only 3 minutes reduction and went up to ω=0.98.

When using CH_4 it activated after about 20 cycles and for CO it was faster, as it took about 10 cycles. This is in accordance with previous work carried out by Adánez et al. [32], which found that the activation of ilmenite particles is a relatively fast process, and that the number of cycles needed to reach a roughly constant reactivity during TGA experiments did not

depend on the reducing gas used, but on the conversion of the oxygen-carrier reached in each reducing cycle. Ilmenite had a faster activation with CO because ilmenite was further converted in every reduction.

The reduction reactivity of ilmenite during consecutive redox periods was assessed. The representation of the normalized rate index of ilmenite reaction before and after the activation process and for the gases tested (see Figure 6) showed that the reaction rate of ilmenite increased after activation. In case of CH_4 the increase in the reaction rate is greater than with the other gaseous fuels, as the rate index raised here in batch fluidized-bed 5 times after activation. The increase in the rate index for CO and for H_2 was lower as shown by previous studies and it was about 2 times. In the rate index showed not only the oxygen-carrier reactivity is included, but it is also influenced by diffusional limitations in the fluidized bed. The intrinsic kinetics of ilmenite were evaluated in TGA in a previous work [36]. These data obtained in fluidized bed reactor can be easier comparable to previous similar experiments. For example, other iron-based oxygen-carriers previously tested in batch fluidized-bed by Johansson et al. [34] had normalized rate index values with CH_4 within the range of 0.4 to 4%/min. This oxygen-carrier had a rate index slightly lower than 0.4%/min with CH_4, that is, in the lower range of other synthetic Fe-based oxygen-carriers. Nevertheless, the rate index for H_2 was calculated to be above 1.1%/min at the start of the reduction period, which is adequate for the use in CLC with solid fuels [33].

4.2. Reactivity with syngas

Batch experiments were also performed using syngas as fuel, since it is actually the coal gasification product, primarily composed by H_2 and CO. Thus, in CLC with solid fuels syngas

is the main gaseous fuel that reacts with the oxygen-carrier, when coal is previously externally gasified and the product gas is later introduced into the CLC system. A mixture $CO+H_2$ is also the main reacting gas flow when coal is directly introduced in the fuel-reactor and is in situ-gasified.

100 redox cycles with syngas of composition 21.5% H_2 + 28.5% CO + 8% H_2O + 8.2% CO_2 were performed. Very little H_2 in the outlet gas was seen at the beginning of the reducing cycles: about 1-2%. Likewise, the CO content was about 2.4%. Figure 7.a represents the CO_2 concentration profiles obtained and Figure 7.b shows the variation of the oxygen yield with the solids conversion for various reducing periods from the 100 redox cycles.

When focusing only in the first 1.5 minutes of each reducing period, it can be seen that the CO_2 and the oxygen yield increase within the first 10 cycles approximately and reach a maximum value, which is due to the activation of ilmenite. This maximum value is maintained throughout the cycles, which indicates that ilmenite maintains its reaction rate and does not deactivate. This corresponded to a ω of about 0.99. Besides, the oxygen yield obtained was as high as 98%.

On the other hand, after about 1.5 minutes and ω further than 0.99, there was a decrease in the produced CO_2 and in the oxygen yield. This was not due to a deactivation of ilmenite, but to a decrease in the oxygen transport capacity. In previous work, Adánez et al. [32] found that the Fe_2TiO_5 present in the ilmenite undergoes a physical segregation with the number of cycles and separated Fe_2O_3 and TiO_2 are formed, which reduce the oxygen transport capacity, R_{OC}, of ilmenite. This fact will be deeply discussed later. Figure 7.b shows that the oxygen yield reached after many cycles was close to the corresponding γ_O for the $Fe_3O_4 \leftrightarrow FeO$ equilibrium.

Various syngas ratios

Additional redox cycles with different H_2:CO ratios were also done with the same activated ilmenite after the 100 cycles with syngas. Different H_2:CO ratios from 100:0 to 0:100 have been tested. As well as in the previous tests with syngas, H_2O and CO_2 were introduced to accomplish the water-gas shift equilibrium at 1173 K for every mixture.

In Figure 8.a the variation along the reducing cycle of the calculated normalized rate index for H_2, CO and the syngas mixtures as a function of ilmenite mass based conversion are shown. It can be seen that the reaction rate was higher for the experiments carried out with H_2 and the lower values were obtained when using only CO. A dotted line is drawn at ω of 0.99 because it was previously seen that until that conversion the reaction rate and oxygen yield were maintained constant and had maximum values that decreased when ilmenite was further converted.

Figure 8.b represents the average rate index as a function of the fraction of H_2 in the reducing agent, together with a dotted line, which is a theoretical rate index calculated as sum of the rate index of H_2 and CO multiplied per their corresponding fractions. It can be seen that the resulting reaction rates for all syngas mixtures tested matches with the theoretical line. It can be thereby concluded that the reaction rate for a syngas mixture can be actually calculated as the sum of both reducing agents reaction rates.

4.3. Reactivity in oxidation

Ilmenite had undergone an activation process for the reduction reaction after a low number of cycles and depending on the conversion variation reached in each cycle. The oxidation reaction is a two step reaction [36]: the first step is controlled by chemical reaction and the second is controlled by the diffusion. The first step of the reaction was also fast activated after a low number of redox cycles. Figure 9 represents the O_2 profiles obtained during the first oxidation periods in the above mentioned 100 redox cycle test performed in the batch fluidized-bed. The oxidation gas is diluted air in N_2 with 10% O_2. At the beginning of the oxidation period no oxygen could be seen in the produced gas, since it reacted with ilmenite, re-oxidizing it. After this period, the breakthrough curve of oxygen appeared, which is different depending on the reactivity of the bed material [37]. The profiles show that the slope increased significantly with the number of cycles, which was due to the activation process and increase in the reaction rate that was later proven with TGA analysis. The activation took about 8 cycles.

Figure 10 shows the O_2 profiles for the oxidation periods, from cycles 20 to 100. The slope rose slightly with the number of cycles and it took longer for oxygen to appear. The second step of reaction, controlled by diffusion, appeared later for higher oxidizing conversions. This was because of the increase in the porosity of the oxygen-carrier. When ilmenite was completely activated for the oxidation reaction, the diffusion did not control the reaction any more.

It could be also observed that if the surface under the O_2 curve was integrated, the oxygen amount taken by ilmenite with the number of cycles was slight but gradually decreasing. That is because the ilmenite was in the previous reducing period less reduced, as the oxygen transfer capacity was gradually decreasing, as will be later discussed.

4.4. Physical and chemical changes in ilmenite particles throughout the redox cycles

The major change with respect to the initial ilmenite was that porosity increased substantially with the redox cycles. For the 100 cycle test using syngas as reducing agent, the initial porosity of calcined ilmenite was measured to be 1.2%, after 8 cycles it increased to 12.5%, after 20 cycles it was 27.5% and after 100 cycles it reached the value of 38%.

Final BET measurements for activated ilmenite: with CH_4, after 23 cycles: 0.4 m^2/g; with CO, after 20 cycles: 0.6 m^2/g, and with $CO+H_2$ mixture: 0.4 m^2/g. The initial calcined ilmenite had a BET surface of 0.8 m^2/g. The BET surface in ilmenite in all cases and thus the microporosity is negligible in this material. Macropores are considered to be bigger than 50 nm and the pore distribution shown in Figure 11 confirms that the minimum pore size is about 30 nm, but as porosity increases, the pore distribution locates in higher pore diameters and the average pore diameter gradually increases with the number of cycles and higher pores are formed. In order to explain this gradual increase in porosity, a morphological characterization of samples taken from the 100 redox cycle experiment was done by SEM.

Figure 12 shows SEM microphotographs that confirm the low pore development for calcined ilmenite. The final porosity after 100 redox cycles was 38%. Throughout the reduction-oxidation cycles, there is continuous appearance of cracks, which generate the mentioned rise in porosity. Moreover, a gradual generation of an external layer slightly separated from the rest of the particle which grows with the number of cycles could be clearly observed. This space between the layer and the core also enhances the porosity measured for the particle.

EDX analyses were done to determine Fe and Ti distributions throughout the particles. In calcined ilmenite both distributions were uniform, what agrees with the XRD analysis that reveals Fe_2TiO_5 as main component. However with the number of cycles Fe_2TiO_5 has been seen to undergo a physical segregation and the particle core gets titanium enriched, whereas the external part gets iron enriched. XRD analyses to the external layer found that this region is composed only by iron oxide, whereas XRD to the internal core revealed the existence of TiO_2 and Fe_2TiO_5. After each cycle there is more free TiO_2 in the core and iron oxide in the external shell, together with a decrease of iron titanates. That means that there is a migration phenomenon of iron oxide towards the external part of the particle, where there is not TiO_2 to form iron titanates. Since the active phase for a CLC application is the iron oxide, the fact that iron oxide is at the outer part of the solid facilitates the reaction.

Initial and activated ilmenite after 20 cycles particles have relatively high values of crushing strength, it varied from 2.2 N to 2.9 N. These values for the crushing strength would be acceptable for the use of these particles in circulating fluidized-bed [34]. Crushing strength measures were made for fully oxidized as well as fully reduced samples of ilmenite activated with CO. Both samples have a similar value for crushing strength around 2.9. However, particles after 50 and 100 cycles show a decreased crushing strength down to a value of 1 N after 100 cycles. 1 N is a border value for the use of a material in fluidized-bed. Nevertheless, as it was previously stated, since there is formation of an external layer, the normal strength under which the particles are subjected could break this layer and not the whole particle.

Maximum oxygen yields and oxygen transport capacity, R_{OC}

Several thermodynamic calculations were carried out to evaluate the maximum oxygen yield, γ_O, at equilibrium conditions. Ilmenite needs special attention due to their composition and the final oxidation states during reduction reaction to reach full conversion of fuel gases towards H_2O and CO_2. In the fully oxidized ilmenite, the iron was found to be as Fe^{III}, either in the Fe_2TiO_5 compound or as free Fe_2O_3. Both compounds have different thermodynamic properties for the reduction reaction. Fe^{III} in Fe_2TiO_5 can be reduced to Fe^{II} in $FeTiO_3$ via the compound $Fe_3Ti_3O_{10}$ [29], which corresponds to $Fe_3O_4 \cdot 3TiO_2$. Table 3 shows the maximum oxygen yields at equilibrium conditions for every step in the reduction reaction mechanism. Thermodynamic calculations show that by reducing Fe_2TiO_5 with CH_4, H_2 or CO it is possible to reach very near full combustion of fuel gas into H_2O and CO_2 when it is reduced into $Fe_3O_4 \cdot 3TiO_2$ and $FeTiO_3$, i.e. γ_O can be considered 1 for practical purposes. Further reduction to Fe^0 is prevented in a CLC system to avoid low fuel gas conversion. However, the reduction of free Fe_2O_3 must be limited to Fe_3O_4 because further reduction to FeO or Fe would produce low values of oxygen yield, γ_O, and therefore, a high increase in the equilibrium concentrations of H_2 and CO exiting from the fuel-reactor. Therefore, Fe^{III} should be reduced as maximum to a mixture of $FeTiO_3$ and Fe_3O_4 in order to get full fuel gas combustion in a CLC system. This condition corresponds to a value for R_{OC} of 4.0% for calcined ilmenite. That means, if more oxygen was transferred and therefore further conversion than $\omega = 0.96$ was reached for that sample, significant amounts of Fe^{II} as FeO would be formed.

Adánez et al. [32] saw that ilmenite undergoes a segregation process with the redox cycles that generates more free Fe_2O_3 and less Fe_2TiO_5. As the oxygen transport capacity for free Fe_2O_3 is lower ($R_{o,Fe2O3} = 3.3\%$) than the oxygen transport capacity for Fe_2O_3 as iron titanate

($R_{o,Fe2TiO5}$ = 6.7%), the gradual separation of Fe_2O_3 from TiO_2 causes a slight and gradual decrease of the oxygen transport capacity of ilmenite with the cycle number.

This decrease in Roc could be clearly seen in the 100 cycle test. Figure 14 is a representation of the R_{OC} measured by TGA of several samples after different number of cycles. The mass variations of the samples were measured when reducing them with 5%H_2 + 40%H_2O. In these conditions it is ensured that the final reduced species are $FeTiO_3$ + Fe_3O_4. XRD analyses of the samples were also done and semi-quantitative analyses measured the free Fe_2O_3 and Fe_2TiO_5 content in the samples. The here called "theoretical R_{OC}" is defined as the oxygen transport capacity that would have the ilmenite sample if the measured free Fe_2O_3 got reduced to Fe_3O_4 and the Fe_2TiO_5 got reduced to $FeTiO_3$. Figure 14 also includes the calculated values of $R_{OC\ theo}$, which are in concordance with the measured R_{OC}. The oxygen transfer capacity, R_{OC}, decreased with the number of cycles. The initial R_{OC} is 4.0% and after 100 redox cycles it was measured to be 2.1%. The main consequence of ilmenite being more reactive with the number of cycles is that with the time fewer inventories are necessary. On the other hand, the decrease in R_{OC} causes the need of higher solid circulating flows between reactors.

However, the decrease in the oxygen transport capacity is not influenced by the reducing agent used, but it depends on the extent of conversion reached in every cycle [32]. Table 4 shows the measured oxygen transport capacity after 20 cycles for the experiments with the gaseous fuels tested, i.e, CH_4, CO and H_2, as well as the average conversion ω reached after every reducing cycle. In all cases ilmenite had undergone the activation period.

If a simplified linear regression is established, the R_{OC} in the 20th cycle could be calculated as $R_{OC}(20^{th}) = (37.5 \cdot \omega - 36.017) \cdot R_{OC,ini}$, being $R_{OC,ini}$ the initial oxygen transport capacity, which for this ilmenite was 4.0%.

The effect of ilmenite activation on the performance of a CLC system was already investigated by Adánez et al. [32] because there is a trade-off between the increase in reactivity and the decrease in the oxygen transport capacity. However, the R_{OC} values showed for initial, activated ilmenite and after a high number of redox cycles are high enough values to transfer the required oxygen from air to fuel in a CLC system [38]. Furthermore, the performance in continuous testing showed that the oxygen transport capacity of ilmenite decreased very little, because the extent of conversion reached in the fuel-reactor was not high [27].

4.5. Carbon formation and fluidizing behavior

4.5.1. Carbon formation

The deposition of carbon from carbon containing gases is a concern because it can deactivate the oxygen-carrier or diminish its oxygen transfer. It can also cause defluidization problems. Besides, if carbon is formed, it can be further directed to the air-reactor where it will be burnt, being therewith the carbon capture efficiency decreased. Carbon formations in CLC processes have been already seen and studied with different oxygen-carriers [39,40]. There are two possible ways of carbon formation: through methane decomposition or through Boudouard reaction. The conditions for which carbon formation is thermodynamically possible in the

CLC process depend on the amount of oxygen added with the oxygen-carrier as well as the temperature and pressure.

If there was carbon formation when using carbon-containing fuel gases, i.e. CH_4 and CO, there would be some CO or CO_2 release during the oxidizing periods due to the oxidation of the carbon. However, no CO and CO_2 were observed any time during inert or oxidation periods, indicating that there was not accumulation of carbon during reduction periods in any of the experiments carried out.

4.5.2. Particle integrity and attrition

The attrition rate of the carriers is an important parameter to be accounted as a criterion for using a specific oxygen-carrier in a fluidized-bed reactor. High attrition rates will decrease the lifetime of the particles increasing the reposition of the oxygen-carrier in the CLC system. Particles elutriated from the fluidized-bed reactor were retained in a filter, and were taken every 10 cycles. The loss of fines was considered as the particles with a diameter under 40 μm, because they are the particles that could only be recovered in cyclones with separation efficiency higher than 99% [41]. Ilmenite showed low attrition rates. 100 redox cycles were done in 56 hours of performance in fluidizing conditions. Figure 15 shows the fine attrition rate (particle size below 40 μm) as a function of fluidization time. The initial value of attrition at the beginning is due to the rounding off of angular initial ilmenite particles. With the number of cycles, an external layer was seen to be formed, as it can be seen in Figure 12, and that this layer is mainly composed by iron oxides. The initial formation of this layer could explain the higher values of fines formed around 20 hours. After 40 hours of operation the attrition rate stabilized to a value of 0.064%/hour. Furthermore, XRD analysis of fines

showed that they are formed only by iron oxide, and titanium oxide or iron titanates were not observed. This fact suggests that fines are produced by an attrition process in the particle surface, and not by the breakage of particles. There is particle rounding and detachment of part of the external layer, but no particle fragmentation.

4.5.3. Defluidization

The behavior of ilmenite with respect to particle agglomeration in the fluidized-bed has been also analyzed in this work. Particle agglomeration must be avoided because it can lead to bed defluidization that causes solids circulation disturbances and channeling of the gas stream through the bed, which turns the contact between gas and particles less efficient. During the experimental tests, defluidization problems were never observed. Moreover, particles extracted from the fluidized-bed at the end of the tests did not show agglomeration evidences. However, the extent of reduction during the experiments was limited to $\omega = 0.98$. To check if agglomeration problems could appear at higher conversion levels, ilmenite was reduced during longer periods. The particles used were the just activated with H_2 from experiment 3. Reduction time was gradually increased in successive redox cycles. Defluidization appeared during the oxidation period and when the mass based conversion was about 0.97. For such conversions some free Fe_2O_3 would get reduced up to FeO, regarding the thermodynamics. The appearance of defluidization problems by oxidation of FeO was previously found by Cho et al. [39] for iron-based oxygen-carriers supported on alumina. This also agrees with the fact found by Leion et al. [29] that ilmenite presents an agglomeration risk at high conversions. However, FeO formation in a CLC system should be avoided because thermodynamic limitations. Furthermore, Abad et al. [38] concluded that for the optimization of the CLC process it is necessary to get to a compromise between the solids circulation and the solids

inventory. The optimum values of the conversion variation in the fuel-reactor to get low circulation rates and low solids inventory could be about 0.2–0.4 because higher values highly increase the solid inventories. Therefore, agglomeration of ilmenite particles is not expected at these conditions if ilmenite reaches a high oxidation degree in the air-reactor.

5. Conclusions

The activation process of ilmenite through consecutives redox cycles in a fluidized-bed reactor has been analyzed. CH_4, H_2 or CO were used as reducing gases. Ilmenite increased its reactivity with the number of cycles, especially for CH_4. Ilmenite activation process depended on the reduction conversion reached in every cycle, being faster activated when the conversion was higher. Reaction with H_2 is faster than with CO, and near full H_2 conversion was obtained in the fluidized-bed reactor. Lower reactivity was found for CH_4, being CH_4 the most unconverted gas. In this case, negligible amounts of H_2 or CO were observed, indicating that CH_4 reforming reaction has low relevance in this system.

For all gaseous fuels tested the reaction rate was maximum and constant at the beginning of the reducing period until an ilmenite mass conversion of about 0.99 and that this value did not decrease for a high number of redox cycles, i.e, 100 cycles. For a conversion further than 0.99, there was a decrease in the oxygen yield that was not due to a deactivation of ilmenite, but to a decrease in the oxygen transport capacity with the redox cycles. The oxygen yield reached after many cycles was close to the corresponding for the $Fe_3O_4 \leftrightarrow FeO$ equilibrium.

For mixtures with different H_2:CO ratios it was seen that reaction rate for a syngas mixture can be calculated as the sum of both reducing agents reaction rates.

The oxidation reaction was also studied. For a conversion of 0.975 in the previous reduction periods, the activation in the oxidation reaction took about 8 cycles. The second step of reaction, controlled by diffusion, appeared later and for higher oxidizing conversions for higher number of cycles and when ilmenite was completely activated for the oxidation reaction, the diffusion did not control the reaction any more. This was because of the increase in the porosity of the oxygen-carrier. The oxidation reaction was fast and fully oxidized ilmenite was reached in every cycle. With the number of cycles the oxygen amount taken by ilmenite was slight but gradually decreasing because of the decrease in the oxygen transfer capacity.

Structural changes on the ilmenite particles after activation were observed. Initial ilmenite particles had low porosity of 1.2% and the porosity of the particles after 100 cycles increased up to 38%. The appearance of an external shell in the particle was observed, which is Fe enriched. As activation proceeds the reactivity increased, but the oxygen transport capacity decreased due to the appearance of free Fe_2O_3 in the external shell. Thus, the initial R_{OC} value is 4.0% and it decreased until 2.1% after 100 redox cycles. A relation between the oxygen transport capacity decrease and the extension of reduction was calculated.

Low attrition values were found during fluidized-bed operation, and no defluidization was observed for typical operating conditions in a CLC process.

Acknowledgments

This work was partially supported by the European Commission, under the RFCS program (ECLAIR Project, Contract RFCP-CT-2008-0008), from Alstom Power Boilers and by the

Spanish Ministry of Science and Innovation (Project ENE2010-19550). A. Cuadrat thanks CSIC for the JAE Pre. fellowship. Alberto Abad thanks to the Ministerio de Ciencia e Innovación for the financial support in the course of the I3 Program.

Nomenclature

CLC Chemical-Looping Combustion

F_{in} molar flow of the inlet gas stream (mol/s)

F_{out} molar flow of the outlet gas stream (mol/s)

Me_xO_y oxidized form of the oxygen-carrier

Me_xO_{y-1} reduced form of the oxygen-carrier

M_O molecular mass of oxygen (kg/mol)

m_{ox} mass of the most oxidized form of the oxygen-carrier (kg)

m_{red} mass of the reduced form of the oxygen-carrier (kg)

P_{in}, P_{out} partial pressures of the gaseous fuel at the reactor inlet and outlet, respectively

P_{ref} reference partial pressure

$r_0(t)$ rate of oxygen transferred (mol O/s)

R_{OC} oxygen transport capacity of the oxygen-carrier

$R_{OC\ theo}$ theoretical oxygen transport capacity of the oxygen-carrier

T temperature (K)

$t_{r,0}$ initial time when the considered reaction begins (s)

x_i molar fraction of the gas i

X_{max} maximum CO_2 or H_2O corresponding fraction if full combustion was reached

ε_g coefficient of expansion of the gas mixture

γ_O oxygen yield

ω mass based conversion of ilmenite in the fluidized-bed

$\omega_{f,red}$ final conversion of ilmenite reached in the previous reduction

$\left(d\omega/dt\right)_{exp}$ experimental rate of conversion (kg O/(s·kg oxygen-carrier))

Bibliography

[1] Climate Change 2007: Synthesis Report. Contribution of Working Groups I, II and III to the Fourth Assessment Report of the Intergovernmental Panel on Climate Change; Pachauri, R. K., Reisinger, A., Eds.; IPCC: Geneva, CH, 2008.

[2] IEA, International Energy Outlook, 2008 www.eia.doe.gov/iea; 2008.

[3] L.I. Eide, M. Anheden, A. Lyngfelt, C. Abanades, M. Younes, D. Clodic, Novel Capture Processes, Oil & Gas Science and Technology 60 (2005) 497-508.

[4] H. R. Kerr, Capture and separation technologies gaps and priority research need. In Carbon Dioxide Capture for Storage in Deep Geologic Formations - Results from the CO2 Capture Project; Thomas, D., Benson, S., Eds.; Elsevier Science: Oxford, 2005; Vol. 1, Chapter 38.

[5] M.M. Hossain, H.I. de Lasa, Chemical-looping combustion (CLC) for inherent CO2 separation—A review, Chem. Eng. Sci. 63 (18) (2008) 4433-4451.

[6] A. Lyngfelt, B. Leckner, T. Mattisson, A fluidized-bed combustion process with inherent CO2 separation; application of chemical-looping combustion, Chem. Eng. Sci. 56 (2001), 3101–3113.

[7] H.J. Ryu, G.T. Jin, C.K. Yi, Demonstration of inherent CO_2 separation and no NOx emission in a 50 kW chemical-looping combustor: Continuous reduction and oxidation experiment. In Proceedings of the Seventh International Conference of Greenhouse Gas Control Technologies; Wilson, M., Morris, T., Gale, J., Thambibutu, K., Eds.; Elsevier Ltd.: Amsterdam, The Netherlands, 2005; Vol. 2, pp 1907.

[8] P. Kolbitsch, J. Bolhàr-Nordenkampf, T. Pröll, H. Hofbauer, Operating experience with chemical looping combustion in a 120 kW dual circulating fluidized bed (DCFB) unit, International Journal of Greenhouse Gas Control 4 (2) (2010) 180-185.

[9] C. Linderholm, A. Abad, T. Mattisson, A. Lyngfelt, 160 hours of chemical-looping combustion in a 10 kW reactor system with a NiO-based oxygen carrier, International Journal of Greenhouse Gas Control 2 (2008) 520-530.

[10] C. Linderholm, T. Mattisson, A. Lyngfelt, Long-term integrity testing of spray-dried particles in a 10 kW chemical-looping combustor using natural gas as fuel, Fuel 88 (2009) 2083-2096.

[11] L.F. de Diego, F. Garcia-Labiano, P. Gayan, J. Celaya, J.M. Palacios and J. Adanez, Operation of a 10 kWth chemical-looping combustor during 200 h with a CuO–Al_2O_3 oxygen carrier, Fuel 86 (7–8) (2007) 1036–1045.

[12] T. Mattisson, F. García-Labiano, B. Kronberger, A. Lyngfelt, A., J. Adánez, H. Hofbauer, Chemical-looping combustion using syngas as fuel, International Journal of Greenhouse Gas Control 1 (2) (2007) 158-169.

[13] H. Jin, M. Ishida, A new type of coal gas fueled chemical-looping combustion, Fuel 83 (17-18) (2004) 2411-2417.

[14] J. Wolf, M. Anheden, J. Yan, Performance Analysis of Combined Cycles with Chemical Looping Combustion for CO_2 Capture. In International Pittsburg Coal Conference, Newcastle, New South Wales, Australia, Dec 3-7, 2001.

[15] T. Mattisson, F. Garcia-Labiano, B. Kronberger, A. Lyngfelt, J. Adanez, H. Hofbauer, Chemical-looping combustion using syngas as fuel, International Journal of Greenhouse Gas Control, 1 (2007) 158-169.

[16] A. Abad, F. García-Labiano, L.F. de Diego, P. Gayán, J. Adánez, Reduction kinetics of Cu-, Ni-, and Fe-based oxygen carriers using syngas (CO+H2) for chemical-looping combustion, Energy & Fuels 21 (2007) 1843–1853.

[17] C.R. Forero, P. Gayán, L.F. de Diego, A. Abad, F. Garcia-Labiano, J. Adánez, Syngas combustion in a 500 Wth chemical-looping combustion system using an impregnated Cu-based oxygen carrier, Fuel Processing Technology 90 (2009) 1471-1479.

[18] E. Johansson, T. Mattisson, A. Lyngfelt, H. Thunman, Combustion of Syngas and Natural Gas in a 300 W Chemical-Looping Combustor, Chem. Eng. Res. Des. 84 (2006) 819-827.

[19] A. Abad, T. Mattisson, A. Lyngfelt, M. Rydén, Chemical-Looping Combustion in a 300 W Continuously Operating Reactor System Using a Manganese-Based Oxygen Carrier, Fuel 85 (2006) 1174-1185.

[20] A. Abad, T. Mattisson, A. Lyngfelt, M. Johansson, The Use of Iron Oxide as Oxygen Carrier in a Chemical-Looping Reactor, Fuel 86 (2007) 1021-1035.

[21] C. Dueso, F. García-Labiano, J. Adánez, L.F. de Diego, P. Gayán, A. Abad, Syngas combustion in a chemical-looping combustion system using an impregnated Ni-based oxygen carrier, Fuel 88 (12) (2009) 2357-2364.

[22] Y. Cao, W.P. Pan, Investigation of chemical looping combustion by solid fuels. 1. Process Analysis. Energy & Fuels 20 (5) (2006) 1836–1844.

[23] J.S. Dennis, S.A. Scott, A.N. Hayhurst, In situ gasification of coal using steam with chemical looping: a technique for isolating CO2 from burning a solid fuel Journal of the Energy Institute, 79 (3) (2006) 187-190.

[24] N. Berguerand, A. Lyngfelt, Chemical-looping combustion of petroleum coke using ilmenite in a 10 kWth unit-high-temperature operation, Energy & Fuels 23 (10) 5257-5268.

[25] N. Berguerand, A. Lyngfelt, The Use of Petroleum Coke as Fuel in a 10 kWth Chemical-Looping Combustor, International Journal of Greenhouse Gas Control 2 (2008) 169-179.

[26] N. Berguerand, A. Lyngfelt, Design and operation of a 10 kWth chemical-looping combustor for solid fuels – Testing with South African coal, Fuel 87 (2008) 2713-2726.

[27] A. Cuadrat, A. Abad, F. García-Labiano, P. Gayán, L.F. de Diego, J. Adánez, The use of ilmenite as oxygen-carrier in a 500 Wth Chemical Looping Coal Combustion unit, Submitted for publication.

[28] A. Bidwe, C. Hawthorne, F. Mayer, A. Charitos, A. Schuster, G. Scheffknecht, Use of Ilmenite as Oxygen-carrier in Chemical Looping Combustion-Batch and Continuous Dual Fluidized Bed Investigation. GHGT-10, Amsterdam, 19-23 September 2010 (expected to be published in Energy Procedia).

[29] H. Leion, A. Lyngfelt, M. Johansson, E. Jerndal, T. Mattisson, The use of ilmenite as an oxygen carrier in chemical-looping combustion, Chemical Engineering Research and Design 86 (2008) 1017-1026.

[30] H. Leion, T. Mattisson, A. Lyngfelt, Solid Fuels in Chemical-Looping Combustion, International Journal of Greenhouse Gas Control, 2 (2008) 180-193.

[31] T. Pröll, K. Mayer, J. Bolhàr-Nordenkampf, P. Kolbitsch, T. Mattisson, A. Lyngfelt, Natural minerals as oxygen carriers for chemical looping combustion in a dual circulating fluidized bed system. GHGT-9: 9th International Conference on Greenhouse Gas Control Technologies, 16–20 November; 2008.

[32] J. Adánez, A. Cuadrat, A. Abad, P. Gayán, L.F. de Diego, F. García-Labiano, Ilmenite activation during consecutive redox cycles in chemical-looping combustion, Energy & Fuel 24 (2010) 1402–1413.

[33] A. Cuadrat, A. Abad, J. Adánez, L.F. de Diego, F. García-Labiano, P. Gayán, Design Considerations for Chemical-Looping Combustion of coal – Part 1. Experimental Tests, Submitted article.

[34] M. Johansson, T. Mattisson, A. Lyngfelt, Comparison of oxygen carriers for chemical-looping combustion, Thermal Science 10 (2006) 93-107.

[35] L.F. de Diego, P. Gayán, F. García-Labiano, J. Celaya, A. Abad, J. Adánez, Impregnated CuO/Al2O3 oxygen carriers for chemical-looping combustion: Avoiding fluidized bed agglomeration, Energy & Fuels 19 (2005) 1850-1856.

[36] A. Abad, J. Adánez, A. Cuadrat, F. García-Labiano, P. Gayán,L.F. de Diego, Reaction kinetics of ilmenite for Chemical-looping Combustion, Chemical Engineering Science, 66 (4) (2011) 689-702.

[37] J. Adánez, A. Abad, F. García-Labiano, L.F. de Diego, P. Gayán, H2S retention with Ca-based sorbents in a pressurized fixed-bed reactor: Application to moving-bed design, Fuel 84 (5) (2005) 533-542.

[38] A. Abad, J. Adánez, F. García-Labiano, L.F. de Diego, P. Gayán, J. Celaya, Mapping of the range of operational conditions for Cu-, Fe-, and Ni-based oxygen carriers in chemical-looping combustion, Chem. Eng. Sci. 62 (2007) 533-549.

[39] P. Cho, T. Mattisson, A. Lyngfelt, Carbon formation on nickel and iron oxide-containing oxygen carriers for chemical-looping combustion, Ind. Eng. Chem. Res. 44 (4) (2005) 668–676.

[40] M. Ishida, H. Jin, T. Okamoto, Kinetic behavior of solid particle in chemical-looping combustion: suppressing carbon deposition in reduction, Energy & Fuels 12 (2) (1998) 223–229.

[41] J.M.Coulson, J.F. Richardson, R.K. Sinnott, Chemical Engineering: Vol. VI. Chemical Engineering Design, Butterworth-Heinemann, Oxford (1997).

Figure captions

Figure 1. Reactor scheme of the CLC process with solid fuels.

Figure 2. Experimental setup used for multicycle tests in a fluidized-bed reactor.

Figure 3. Profiles of CO_2 or H_2O fractions in the product gas (wet basis) during consecutive reduction periods, for a) CH_4, b) CO and c) H_2 as reducing gases. The intervals between reducing periods have been removed. X_{max} is the maximum CO_2 or H_2O corresponding fraction if full combustion was reached. Experimental conditions are showed in Table 2. T = 1173 K.

Figure 4. Product gas distribution in wet basis during reduction with CH_4 and subsequent oxidation for the 20^{th} cycle. Reducing gas: 25% CH_4 + 20% H_2O. T = 1173 K. N_2 to balance. Oxidation: 10% O_2.

Figure 5. Oxygen yield, γ_O, as a function of the ilmenite mass based conversion, ω, for the reduction period after 20 redox cycles for reduction with CH_4 (Reducing gas: 25% CH_4 + 20% H_2O), CO (Reducing gas: 50% CO + 20% CO_2) and H_2 (Reducing gas: 50% H_2 + 20% H_2O). T = 1173 K.

Figure 6. Normalized rate index as a function of the ilmenite mass based conversion, ω, for the reduction reactions with CH_4, CO and H_2 with calcined and activated ilmenite. P_{ref} = 0.15. T = 1173 K.

Figure 7. a) $CO_{2\ dry\ basis}$ profiles in the product gas for various reduction periods and b) Oxygen yield, γ_O, variation with the ilmenite mass based conversion for the reduction periods 3, 10, 20, 40, 50, 70, 85, and 100 for a 100 redox cycle test using syngas as reducing agent. Reducing gas: 21.5% H_2 + 28.5% CO + 8% H_2O + 8.2% CO_2. T = 1173 K.

Figure 8. a) Normalized rate index variation along the reducing cycle as a function of ilmenite mass based conversion and b) Average normalized rate index as function of the fraction of H_2 in the reducing gas for different H_2:CO mixtures tested (see conditions in Table 2). T = 1173 K.

Figure 9. O_2 profiles in the product gas for the first subsequent 20 oxidation periods in a 100 redox cycle test. Previous reducing period of 4 minutes (Reducing gas: 21.5% H_2 + 28.5% CO + 8% H_2O + 8.2% CO_2) and purge with N_2 of 2 minutes. Oxidation with 10% O_2 and gas velocity: 23 cm/s. T = 1173 K. The initial solid mass based conversion of the partially reduced ilmenite was about 0.975.

Figure 10. O_2 profile evolution in the product gas for the oxidation period from cycle 20 to cycle 100 Previous reducing period of 4 minutes (Reducing gas: 21.5% H_2 + 28.5% CO + 8% H_2O + 8.2% CO_2) and purge with N_2 of 2 minutes. Oxidation with 10% O_2 and gas velocity: 23 cm/s. T = 1173 K. The initial conversion ω of the partially reduced ilmenite was about 0.975.

Figure 11. Pore distribution of different samples of ilmenite: Calcined with porosity of 1.2%, after 8 cycles, with porosity of 12.5%, after 18 cycles with porosity of 27% and after 100 cycles with porosity of 38%. Ilmenite samples taken after several redox cycles in Batch Fluidized Bed. Reductions with syngas as fuel (see conditions in Table 2). T = 1173K.

Figure 12. SEM-EDX images of cross-cut ilmenite particles a) calcined and after b) 16, c) 50 and d) 100 redox cycles.

Figure 13. Mechanical strength evolution with the number of cycles.

Figure 14. Measured and theoretical R_{OC}. R_{OC} variation with the number of cycles reduction periods 3, 10, 20, 40, 50, 70, 85, and 100 in a 100 redox cycle test using H_2+CO syngas as reducing agent. Reducing gas: 21.5% H_2 + 28.5% CO + 8% H_2O + 8.2% CO_2. T = 1173 K.

Figure 15. Fine attrition rate (particle size below 40 μm) as a function of fluidization time.

Tables

Table 1. Characterization of calcined and activated ilmenite after 20 redox cycles with CO as reducing agent.

Table 2. Experimental conditions during reduction period in the batch fluidized-bed reactor for experiments 1 to 7. Nitrogen to balance. T = 1173 K.

Table 3. Maximum oxygen yields at equilibrium conditions for different reducing gases in presence of Fe_2TiO_5 and Fe_2O_3 at 1173 K.

Table 4. Measured oxygen transport capacity after 20 cycles and corresponding average conversion ω reached after the reducing cycles for the tests with CH_4, CO and H_2 as reducing agents.

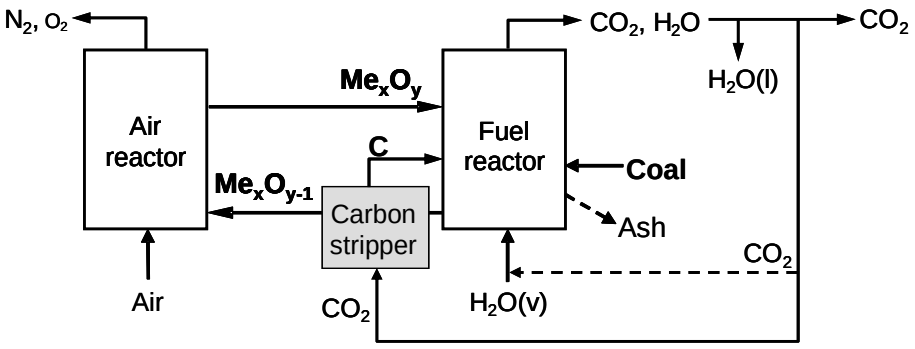

Figure 1. Reactor scheme of the CLC process with solid fuels.

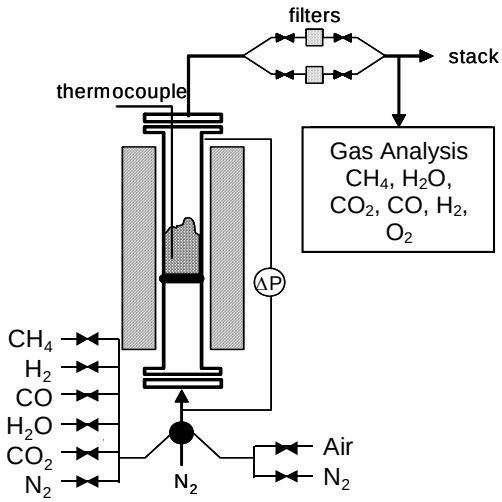

Figure 2. Experimental setup used for multicycle tests in a fluidized-bed reactor.

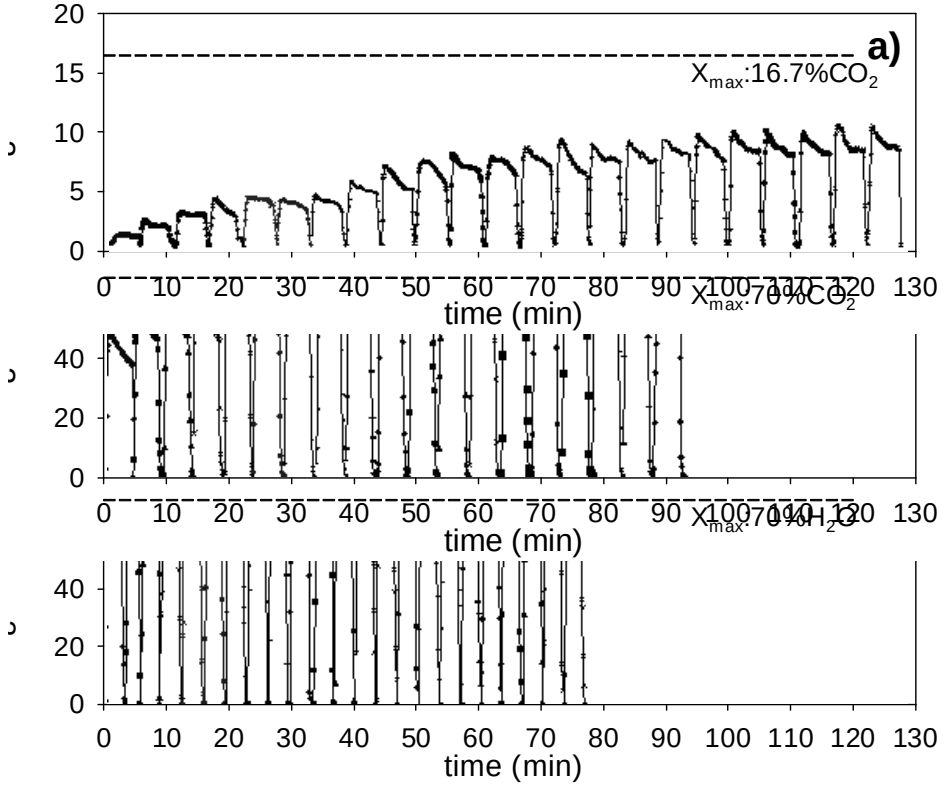

Figure 3. Profiles of CO_2 or H_2O fractions in the product gas (wet basis) during consecutive reduction periods, for a) CH_4, b) CO and c) H_2 as reducing gases. The intervals between reducing periods have been removed. X_{max} is the maximum CO_2 or H_2O corresponding fraction if full combustion was reached. Experimental conditions are showed in Table 2. T = 1173 K.

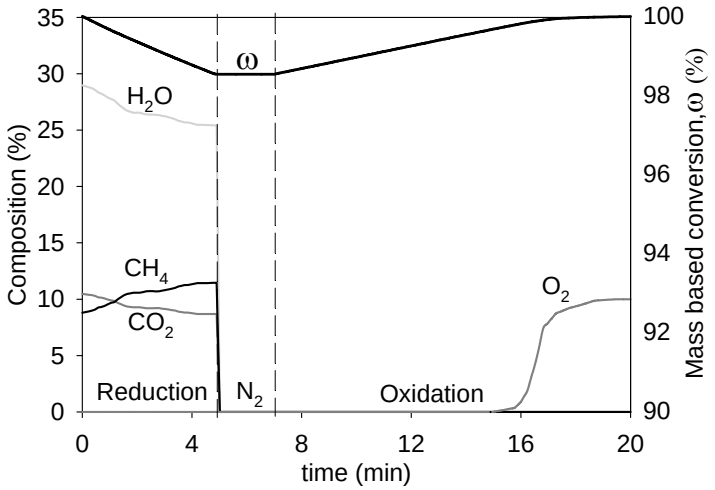

Figure 4. Product gas distribution in wet basis during reduction with CH_4 and subsequent oxidation for the 20th cycle. Reducing gas: 25% CH_4 + 20% H_2O. T = 1173 K. N_2 to balance. Oxidation: 10% O_2.

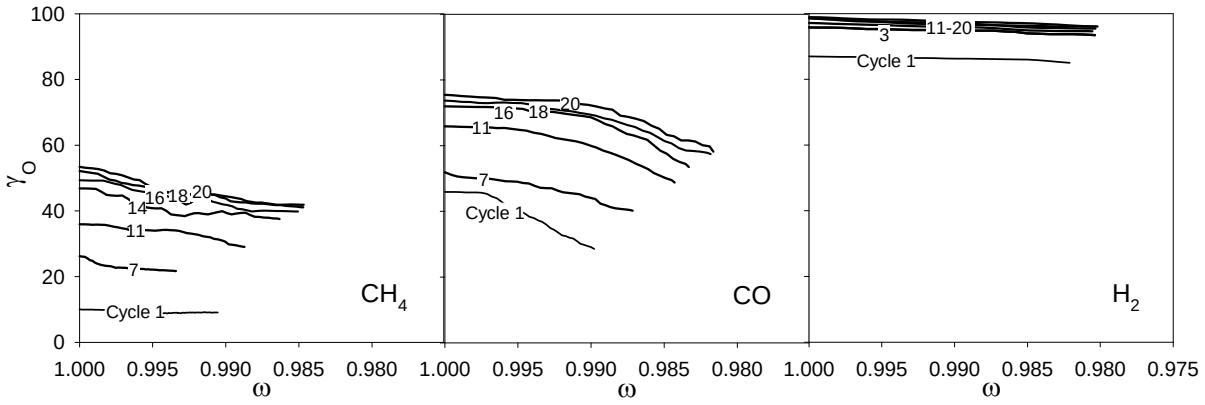

Figure 5. Oxygen yield, γ_O, as a function of the ilmenite mass based conversion, ω, for the reduction period after 20 redox cycles for reduction with CH_4 (Reducing gas: 25% CH_4 + 20% H_2O), CO (Reducing gas: 50% CO + 20% CO_2) and H_2 (Reducing gas: 50% H_2 + 20% H_2O). T = 1173 K.

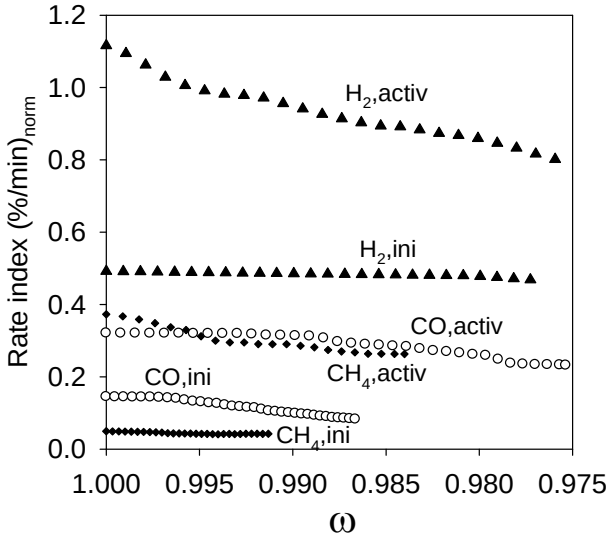

Figure 6. Normalized rate index as a function of the ilmenite mass based conversion, ω, for the reduction reactions with CH_4, CO and H_2 with calcined and activated ilmenite. P_{ref} = 0.15. T = 1173 K.

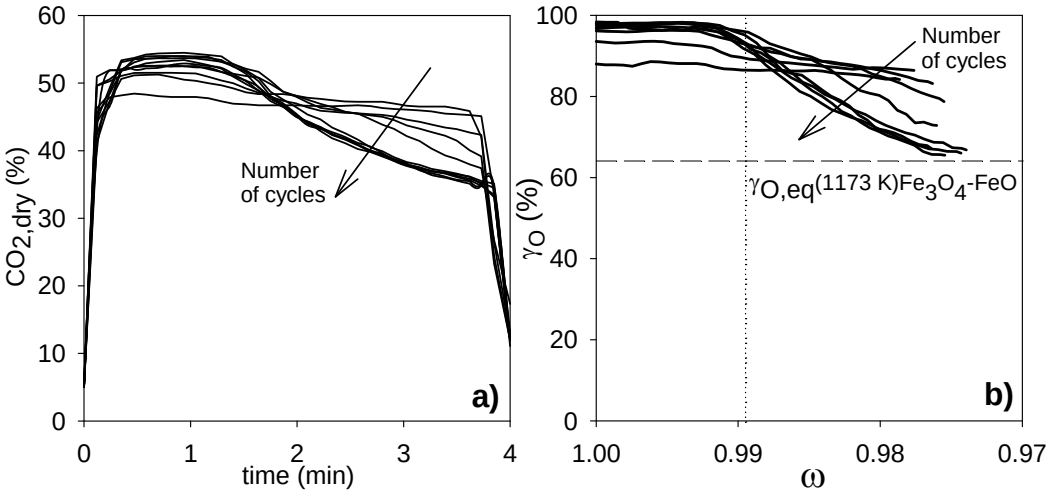

Figure 7. a) $CO_{2\ \text{dry basis}}$ profiles in the product gas for various reduction periods and b) Oxygen yield, γ_O, variation with the ilmenite mass based conversion for the reduction periods 3, 10, 20, 40, 50, 70, 85, and 100 for a 100 redox cycle test using syngas as reducing agent. Reducing gas: 21.5% H_2 + 28.5% CO + 8% H_2O + 8.2% CO_2. T = 1173 K.

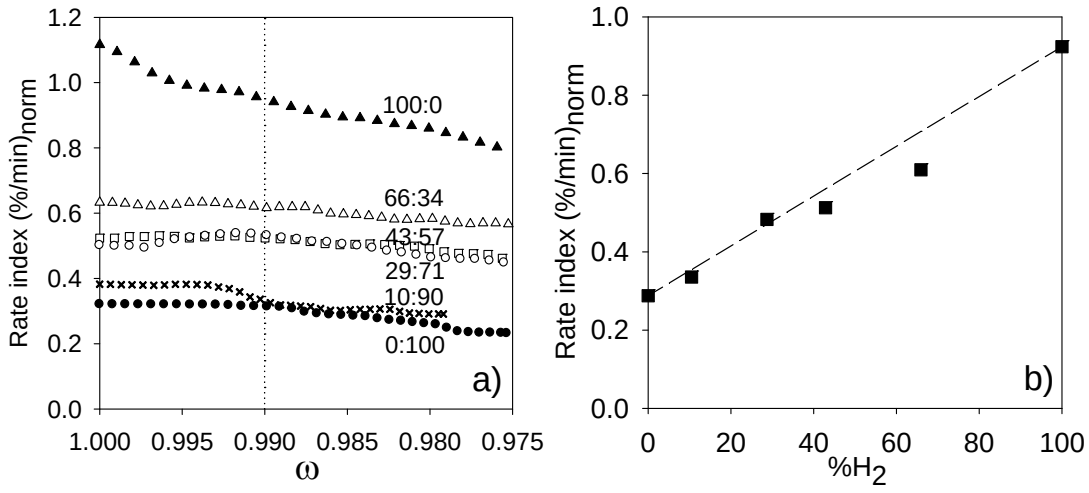

Figure 8. a) Normalized rate index variation along the reducing cycle as a function of ilmenite mass based conversion and b) Average normalized rate index as function of the fraction of H_2 in the reducing gas for different H_2:CO mixtures tested (see conditions in Table 2). T = 1173 K.

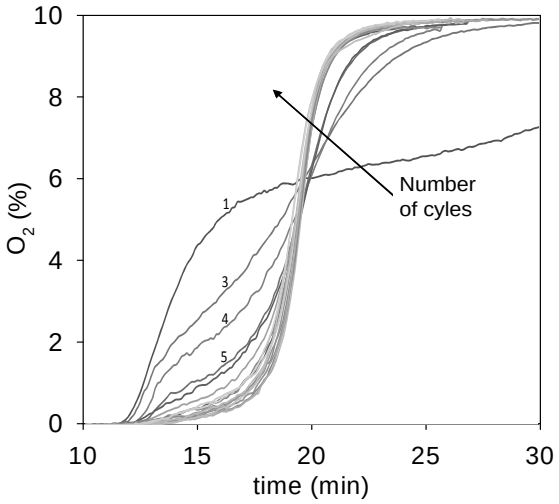

Figure 9. O_2 profiles in the product gas for the first subsequent 20 oxidation periods in a 100 redox cycle test. Previous reducing period of 4 minutes (Reducing gas: 21.5% H_2 + 28.5% CO + 8% H_2O + 8.2% CO_2) and purge with N_2 of 2 minutes. Oxidation with 10% O_2 and gas velocity: 23 cm/s. T = 1173 K. The initial solid mass based conversion of the partially reduced ilmenite was about 0.975.

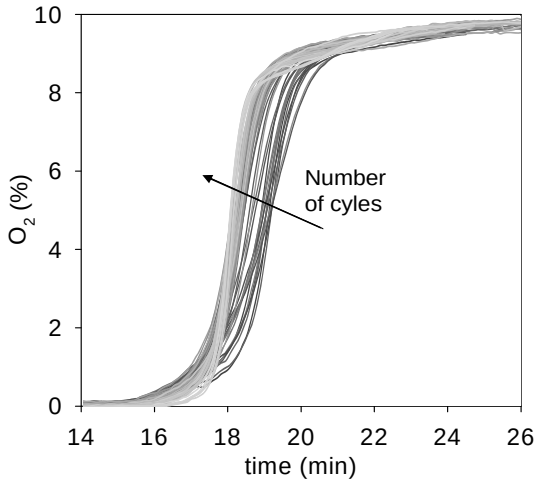

Figure 10. O_2 profile evolution in the product gas for the oxidation period from cycle 20 to cycle 100 Previous reducing period of 4 minutes (Reducing gas: 21.5% H_2 + 28.5% CO + 8% H_2O + 8.2% CO_2) and purge with N_2 of 2 minutes. Oxidation with 10% O_2 and gas velocity: 23 cm/s. T = 1173 K. The initial conversion ω of the partially reduced ilmenite was about 0.975.

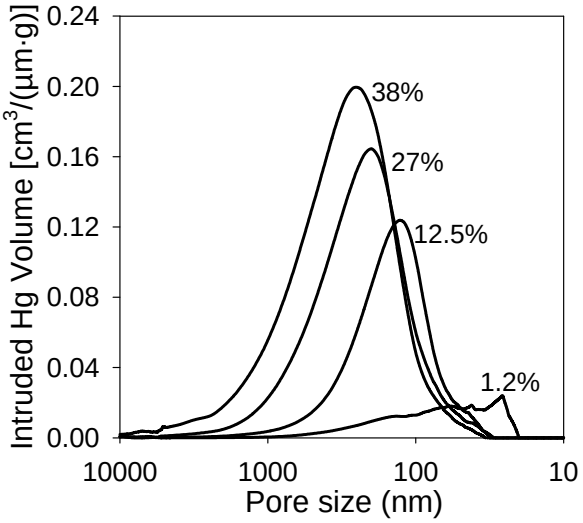

Figure 11. Pore distribution of different samples of ilmenite: Calcined with porosity of 1.2%, after 8 cycles, with porosity of 12.5%, after 18 cycles with porosity of 27% and after 100 cycles with porosity of 38%. Ilmenite samples taken after several redox cycles in Batch Fluidized Bed. Reductions with syngas as fuel (see conditions in Table 2). T = 1173K.

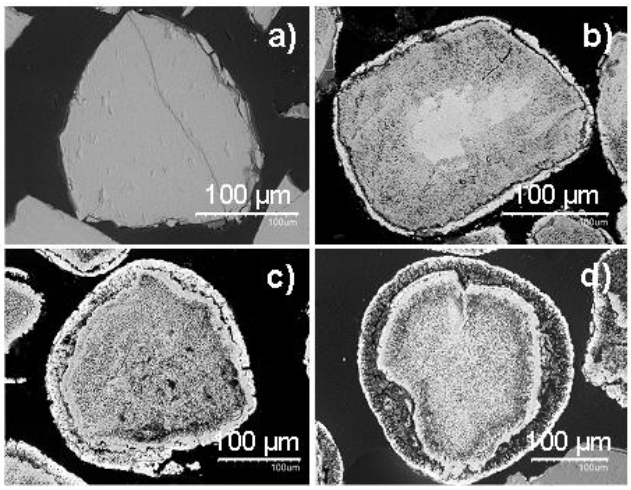

Figure 12. SEM-EDX images of cross-cut ilmenite particles a) calcined and after b) 16, c) 50 and d) 100 redox cycles.

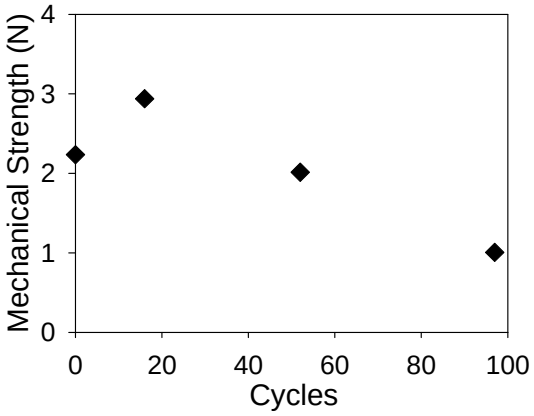

Figure 13. Mechanical strength evolution with the number of cycles.

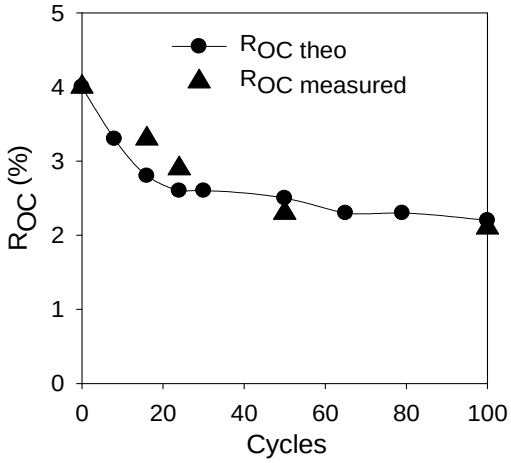

Figure 14. Measured and theoretical R_{OC}. R_{OC} variation with the number of cycles reduction periods 3, 10, 20, 40, 50, 70, 85, and 100 in a 100 redox cycle test using H_2+CO syngas as reducing agent. Reducing gas: 21.5% H_2 + 28.5% CO + 8% H_2O + 8.2% CO_2. T = 1173 K.

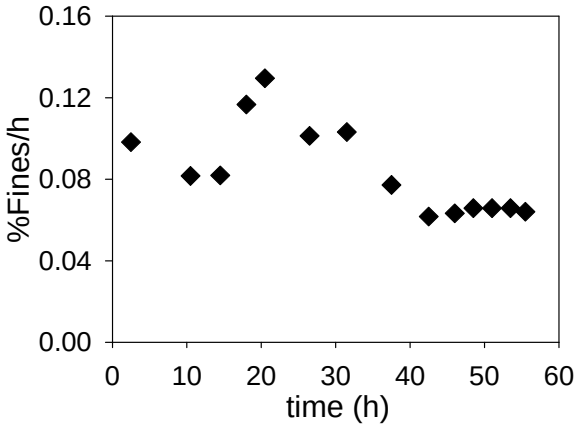

Figure 15. Fine attrition rate (particle size below 40 μm) as a function of fluidization time.

Table 1. Characterization of calcined and activated ilmenite after 20 redox cycles with CO as reducing agent.

	Calcined	**Activated**
Composition by XRD	Fe_2TiO_5,Fe_2O_3,TiO_2	Fe_2TiO_5, Fe_2O_3, Fe_3O_4, TiO_2
Particle diameter (μm)	150-300	150-300
True density (kg/m^3)	4100	4220
Crushing strength (N)	2.2	2.9
Porosity (%)	1.2	27.5
BET Surface (m^2/g)	0.8	0.6

Table 2. Experimental conditions during reduction period in the batch fluidized-bed reactor for experiments 1 to 7. Nitrogen to balance. T = 1173 K.

Exp	Composition (vol%)	Gas velocity (m/s)	Reducing time (s)	Number of cycles	Solids inventory (kg/MW_{th})
1	25% CH_4 + 10% H_2O	0.15	300	23	670
2	50% CO + 20% CO_2	0.3	240	20	480
3	50% H_2 + 20% H_2O	0.3	180	20	560

Exp	Composition (vol%)	H_2O:CO_2	Number of cycles	Solids inventory (kg/MW_{th})
4	33%H_2+17%CO+13.1%H_2O+5.2%CO_2	66 : 34	1	260
5	21.5%H_2+28.5%CO+8%H_2O+8.2%CO_2	43 : 57	100	250
6	14.4%H_2+35.6%CO+10.5%H_2O+20%CO_2	28.8 : 71.2	1	250
7	5.3%H_2+44.7%CO+3.2%H_2O+20.8%CO_2	10.6 : 89.4	1	240

Table 3. Maximum oxygen yields at equilibrium conditions for different reducing gases in presence of Fe_2TiO_5 and Fe_2O_3 at 1173 K.

Oxidized	Reduced	Oxygen yield (γ_O); CH_4	CO	H_2
Fe_2TiO_5	Fe_3O_4+TiO_2	1	1	1
Fe_3O_4+TiO_2	FeO·TiO_2	0.9984	0.9975	0.9981
Fe_3O_4+FeO·TiO_2	Fe_2TiO_4	0.9964	0.9943	0.9956
FeO·TiO_2	Fe+TiO_2	0.3083	0.0849	0.0666
Fe_2O_3	Fe_3O_4	1	1	1
Fe_3O_4	$Fe_{0.947}O$	0.7411	0.6146	0.6748
$Fe_{0.947}O$	Fe	0.5235	0.3246	0.3848

Table 4. Measured oxygen transport capacity after 20 cycles and corresponding average conversion ω reached after the reducing cycles for the tests with CH_4, CO and H_2 as reducing agents.

Reducing agent	R_{OC}(%)	ω
CH_4	3.5	0.984
CO	3.3	0.982
H_2	2.9	0.98